Spectral Entanglement in Entanglement Swapping and Type-I Fusion Gates

Travis S. Humble and Warren P. Grice
Computing and Computational Sciences Directorate
Oak Ridge National Laboratory, Bldg. 5600, MS-6016, Oak Ridge, TN
humblets@ornl.gov, gricew@ornl.gov

Abstract: Correlations in the spectral degrees of freedom affect polarization-based entanglement swapping and type-I fusion gates, with the coherence of the subsequently entangled states essentially and similarly dependent on the initial spectral entanglement.
©2007 Optical Society of America.
OCIS codes: (270.0270) Quantum Optics; (200.0202) Optical Computing

The relative ease with which polarization-entangled photons are generated using spontaneous parametric down-conversion (SPDC) enables immediate realizations of the two-qubit gates underlying many proposals of quantum computation. But the adjunct photonic degrees of freedom can impact this entanglement, e.g., correlated frequencies arising from energy conservation yield spectral entanglement that distinguishes the polarizations. In this paper, we report on the impact of spectral entanglement in the performance of two polarization-encoded two-qubit gates: (1) entanglement swapping [1], which enables offline state preparation in the quantum circuit model [2], and (2) type-I fusion [3], proposed for preparing cluster states in the approach of one-way quantum computing [4].

We consider degenerate type-II SPDC sources to produce polarization-entangled photons pairs (1,2) and (3,4), where the biphoton state of (1,2)

$$\left|\psi_{12}\right\rangle = \frac{1}{\sqrt{2}}\int d\omega \int d\omega' \left[f(\omega,\omega')\left|h_1(\omega), v_2(\omega')\right\rangle + g(\omega,\omega')\left|v_1(\omega), h_2(\omega')\right\rangle \right] \tag{1}$$

is described by the joint spectra $f(\omega,\omega')$ and $g(\omega,\omega')$, i.e., the amplitudes for h_1v_2 and v_1h_2 polarization states, respectively. A similar expression holds for photon pair (3,4). For type-II SPDC, the joint spectra satisfy $f(\omega,\omega') = g(\omega',\omega)$ and, consequently, the marginal spectra correlate with the polarization degree of freedom. The joint spectrum, which is generally inseparable with respect to it's arguments, can be well approximated by a Gaussian distribution having major and minor widths σ_M and σ_m [5], i.e.,

$$f(\omega,\omega') = (\pi\sigma_M\sigma_m)^{-1/2}\exp[-(s\Delta\omega - c\Delta\omega')^2/2\sigma_M^2 - (c\Delta\omega + s\Delta\omega')^2/2\sigma_m^2]. \tag{2}$$

The difference frequencies $\Delta\omega=\omega-\omega_0$ and $\Delta\omega'=\omega'-\omega_0$ are defined with respect to ω_0, half the pump-pulse energy, and $c=\cos\theta$ and $s=\sin\theta$ are given in terms of the angle θ, which orients the major and minor axes of the Gaussian and defines the marginal bandwidths $\sigma^2=\sigma_M^2c^2+\sigma_m^2s^2$ and $\sigma'^2=\sigma_M^2s^2+\sigma_m^2c^2$. See Fig. 1(a). The spectral entanglement is quantified by the linear correlation $|\chi| = \pm(1-\sigma_M^2\sigma_m^2/\sigma^2\sigma'^2)^{1/2}$ and vanishes for $\theta=0$ or $\sigma_M=\sigma_m$.

Entanglement swapping is implemented by sending photons 2 and 3 to a 50:50 beam splitter whose outputs are subsequently discriminated with respect to polarization before being detected. Certain coincidences between detectors [1] correspond with preparation of photons (1,4) in the polarization-entangled state

$$\rho_{14} = \frac{1}{2}\left\{\left|h_1,v_4\right\rangle\left\langle h_1,v_4\right| + G_{14}\left|h_1,v_4\right\rangle\left\langle v_1,h_4\right| + G_{14}^*\left|v_1,h_4\right\rangle\left\langle h_1,v_4\right| + \left|v_1,h_4\right\rangle\left\langle v_1,h_4\right|\right\}, \tag{4}$$

where the coherence

$$G_{14} = \int d\omega \int d\omega' \int d\omega'' f_{12}(\omega,\omega'')g_{34}(\omega'',\omega')^* \int d\omega''' g_{12}(\omega,\omega''')^* f_{34}(\omega''',\omega') \tag{5}$$

depends on the spectral interference between photons 2 and 3. This result, equivalent to the concurrence of ρ_{14}, is a measure of the polarization entanglement resulting from entanglement swapping. For identical sources, the coherence evaluates to $G_{14} = 2a/(a^2+1)$, which is independent of θ and approaches unity as the aspect ratio $a=\sigma_M/\sigma_m$ approaches 1, i.e., the distribution is circularly symmetric and free of spectral entanglement. See the right panel of Fig. 1.

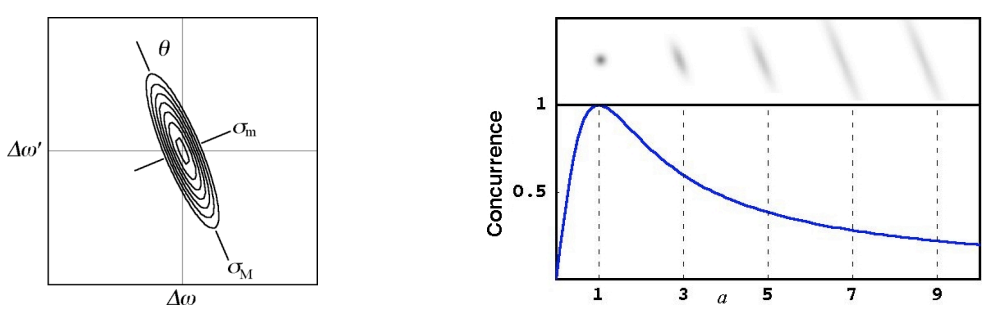

Fig. 1. (left) The rotated Gaussian distribution of Eq. (2). (right) The concurrence resulting from entanglement swapping with respect to the aspect ration $a=\sigma_M/\sigma_m$ and with examples of the joint amplitude shown for $\theta = \pi/8$.

In type-I fusion [3], two pairs of polarization-entangled photon are used as the input to the fusion gate with the intention of generating a three-photon polarization-entangled state. This is accomplished by sending photons 2 and 3 to a polarizing beam splitter after which the polarization of mode 2′ is rotated by π/4. The output in mode 2′ is then discriminated with respect to polarization in the *h*-*v* basis and subsequently detected. For the case of a single-photon detection, e.g., $h_{2'}$, the polarization state of the remaining three-particle state is

$$\rho_{13'4} = \frac{1}{2}\Big\{ |h_1, h_{3'}, v_4\rangle\langle h_1, h_{3'}, v_4| + G_{13'4}|h_1, h_{3'}, v_4\rangle\langle v_1, v_{3'}, h_4| + G^*_{13'4}|v_1, v_{3'}, h_4\rangle\langle h_1, h_{3'}, v_4| + |v_1, v_{3'}, h_4\rangle\langle v_1, v_{3'}, h_4| \Big\}. \quad (8)$$

The coherence is now given by

$$G_{13'4} = \int d\omega \int d\omega' \int d\omega'' f_{12}(\omega,\omega'') f_{34}(\omega'',\omega')^* \int d\omega''' g_{12}(\omega,\omega''') g_{34}(\omega''',\omega')^*, \quad (9)$$

which, like Eq. (5), depends on the spectral interference between photons 2 and 3. However, Eq. (9) differs from Eq. (5), such that, by again considering the sources to be identical, we find

$$G_{13'4} = \frac{4a^2}{(a^2+1)\sqrt{(a^2+1)^2 - (a^2-1)^2 \sin^2 2\theta}}, \quad (10)$$

which depends on both the aspect ratio *a* and the orientation angle *θ*. This result reduces to the previous result for entanglement swapping when *θ*=π/4, i.e., when the two joint spectra are identical. Otherwise, the coherence resulting from type-I fusion is less, as exemplified by the panels of Fig. 2. The left panel demonstrates the dependence of the coherence prepared by fusion as a function of *a* for specific values of the spectra's orientation. Peaks in the right panel of Fig. 3 occur at θ=π/4, an orientation which decouples the spectral and polarization degrees of freedom of Eq. (1). However, the coherence is still less than unity because the photons frequencies remain correlated. It is in principle possible to distinguish the paths that the photons take by monitoring both frequencies. The sole exception is when *a* =1, as then there are no frequency correlations between the photons.

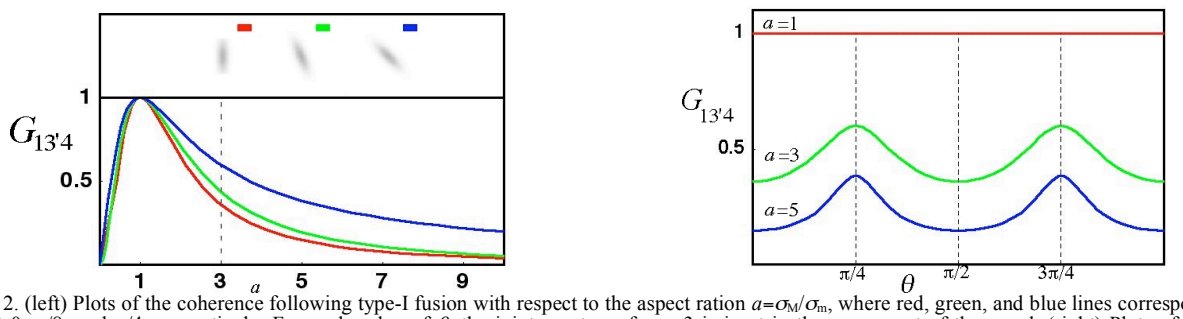

Fig. 2. (left) Plots of the coherence following type-I fusion with respect to the aspect ration $a=\sigma_M/\sigma_m$, where red, green, and blue lines correspond to *θ*=0, π/8, and π/4, respectively. For each value of *θ*, the joint spectrum for *a*=3 is inset in the upper part of the panel. (right) Plots of the coherence with respect to the angle *θ* at fixed values of the aspect ratio.

The performance of the fusion gate can be improved if the polarization of the photon in path 3 is rotated by π/2 prior to the first polarizing beam splitter. In that case, we effectively have $f_{12}(\omega,\omega') = f_{34}(\omega',\omega)$ and the coherence expressed by Eq. (9) evaluates to the expression previously obtained for entanglement swapping, i.e., the result is independent of the angle *θ*, cf. Fig. 1(right). The reason for this change in behavior can be understood to result from the now absent correlations between the spectral and polarization degrees of freedom, i.e., monitoring the frequency of the photon in mode 2′ yields no information regarding the polarizations of the remaining photons. In the previous arrangement, such information was readily available.

The impact of spectral entanglement on the output of these two-qubit gates highlights the need for indistinguishable photons when using quantum-optical approaches to quantum computing. While forethought into the design of the experimental apparatus can sometimes alleviate the impact of spectral entanglement, reductions in polarization entanglement caused by the presence of spectral distinguishability will aggregate as more complicated protocols are carried out, and eventually, either entanglement distillation techniques will be required to (re)purify the states, or the entanglement will be irrevocably lost.

References

1. J.-W. Pan, D. Bouwmeester, H. Weinfurter, and A. Zeilinger, "Experimental entanglement swapping: Entangling particles that never interacted," Phys. Rev. Lett. **80**, 3891 (1998).

2. E. Knill, R. Laflamme, and G. J. Milburn, "A scheme for efficient quantum computation with quantum optics," Nature **409**, 46 (2001).

3. D. E. Browne and T. Rudolph, "Resource-efficient linear optical quantum computation," Phys. Rev. Lett. **95**, 010501 (2005).

4. R. Raussendorf and H. J. Briegel, "A one-way quantum computer," Phys. Rev. Lett. **86**, 5188 (2001).

5. T. S. Humble and W. P. Grice, "Spectral effects in quantum teleportation," submitted (2006).